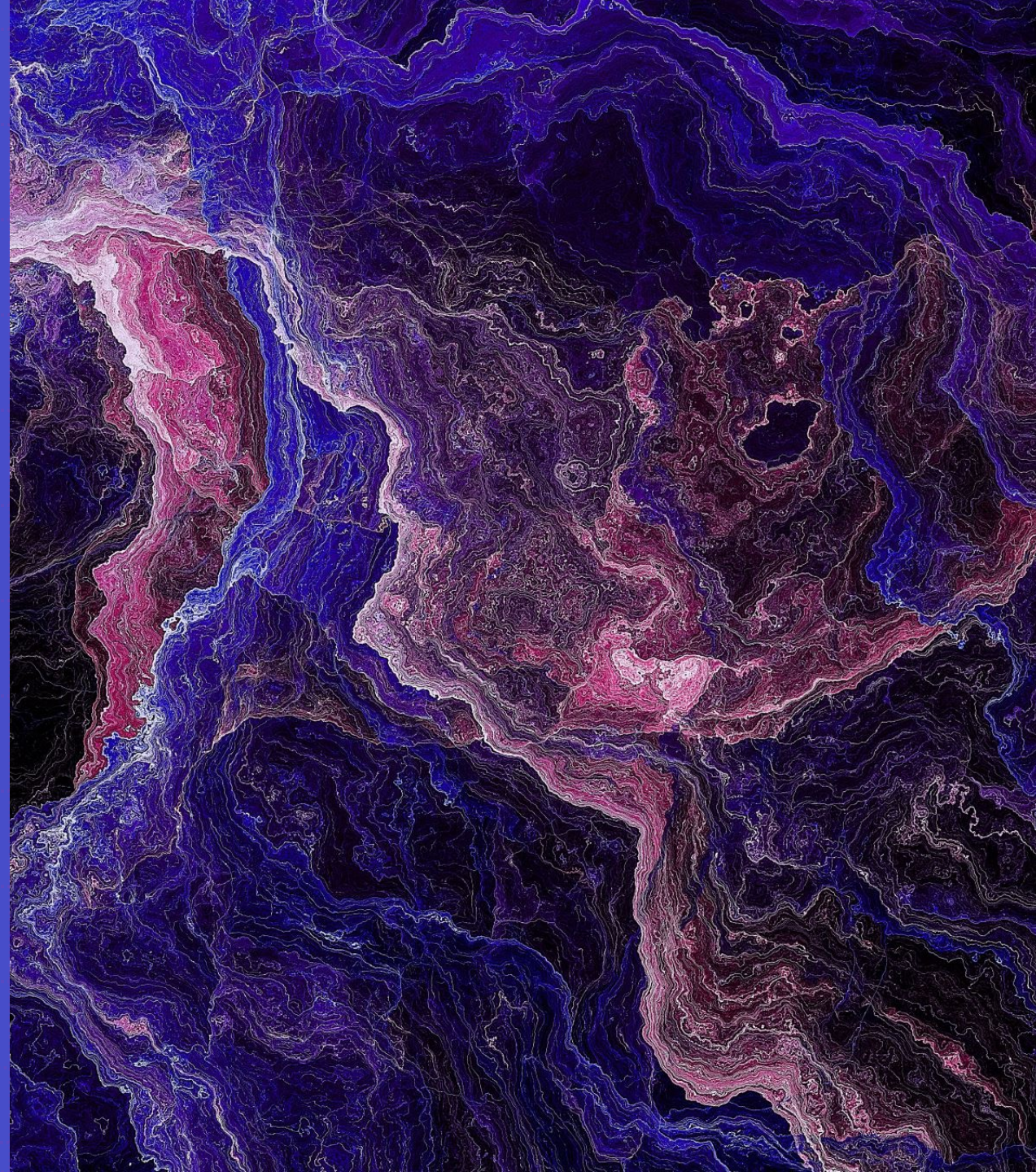
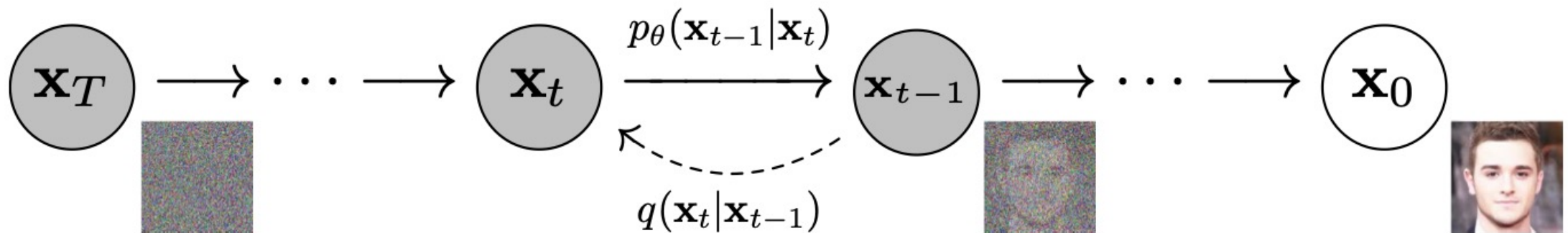


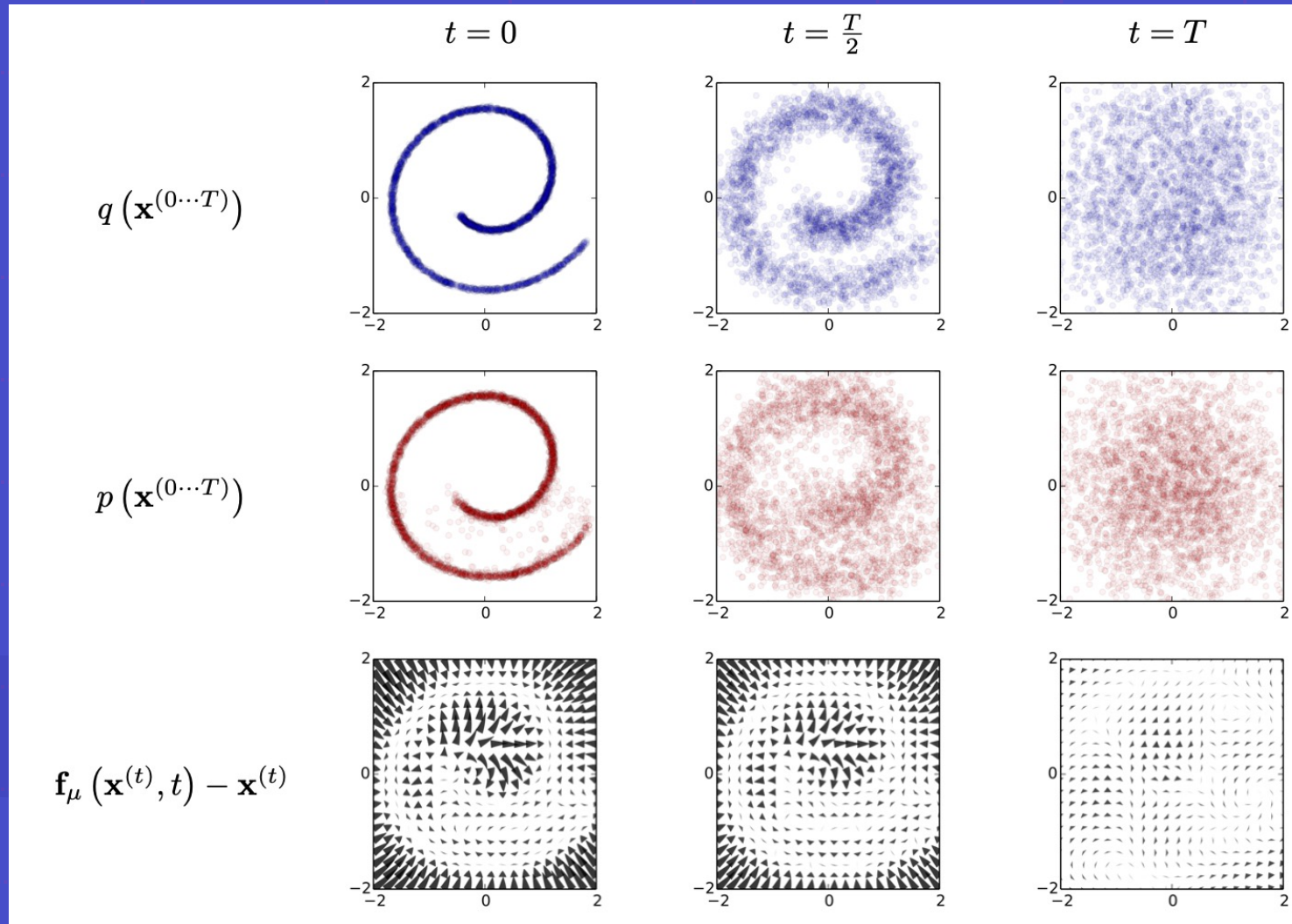
Diffusion models



The markov chain



An example of this process



Forward process (adding noise)

Reverse process

The 'dynamics' / difference

Source: <https://arxiv.org/abs/1503.03585>

Another example

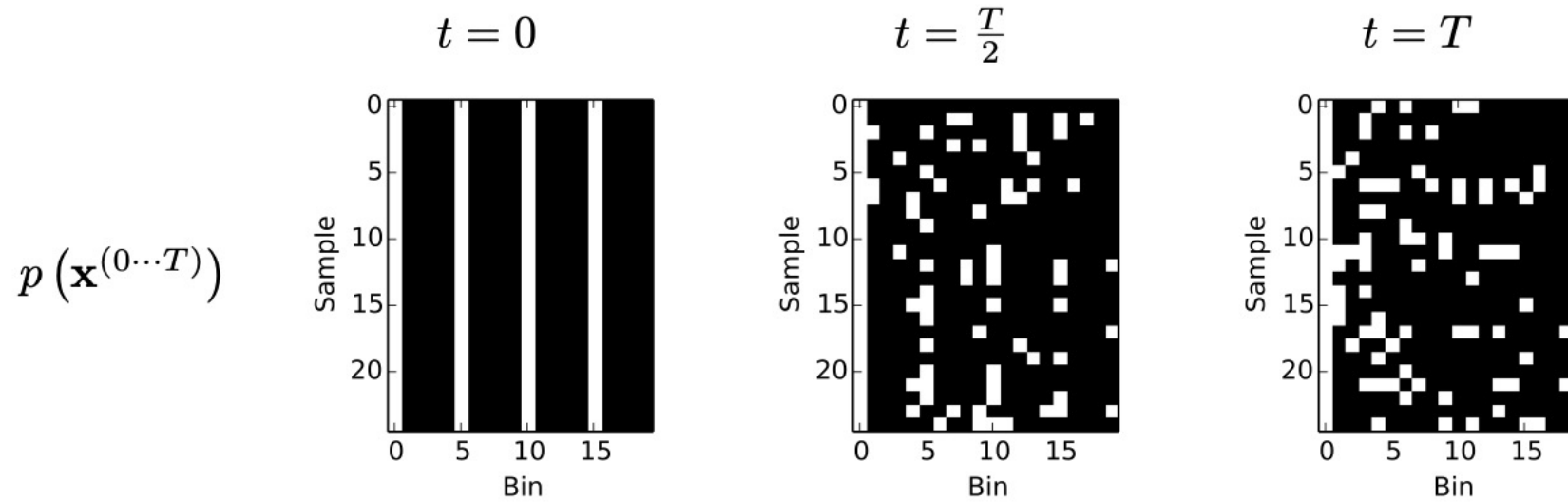


Figure 2. Binary sequence learning via binomial diffusion. A binomial diffusion model was trained on binary ‘heartbeat’ data, where a pulse occurs every 5th bin. Generated samples (left) are identical to the training data. The sampling procedure consists of initialization at independent binomial noise (right), which is then transformed into the data distribution by a binomial diffusion process, with trained bit flip probabilities. Each row contains an independent sample. For ease of visualization, all samples have been shifted so that a pulse occurs in the first column. In the raw sequence data, the first pulse is uniformly distributed over the first five bins.

Similarities with other generative models

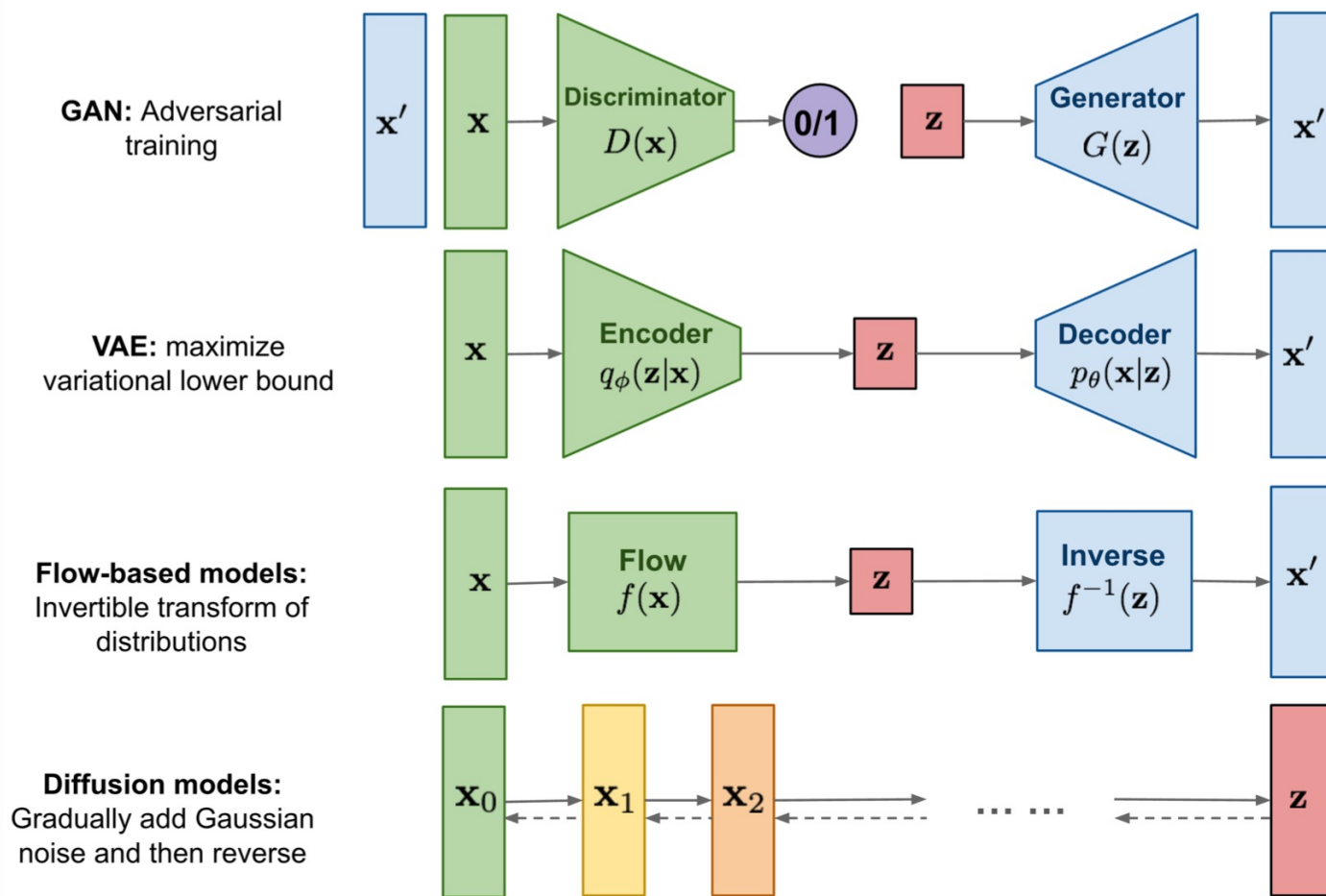


Fig. 1. Overview of different types of generative models.

Source: <https://lilianweng.github.io/lil-log/2021/07/11/diffusion-models.html>

Mathematically

What distinguishes diffusion models from other types of latent variable models is that the approximate posterior $q(\mathbf{x}_{1:T}|\mathbf{x}_0)$, called the *forward process* or *diffusion process*, is fixed to a Markov chain that gradually adds Gaussian noise to the data according to a variance schedule β_1, \dots, β_T :

$$q(\mathbf{x}_{1:T}|\mathbf{x}_0) := \prod_{t=1}^T q(\mathbf{x}_t|\mathbf{x}_{t-1}), \quad q(\mathbf{x}_t|\mathbf{x}_{t-1}) := \mathcal{N}(\mathbf{x}_t; \sqrt{1 - \beta_t}\mathbf{x}_{t-1}, \beta_t\mathbf{I}) \quad (2)$$

Mathematically

The joint distribution $p_\theta(\mathbf{x}_{0:T})$ is called the *reverse process*, and it is defined as a Markov chain with learned Gaussian transitions starting at $p(\mathbf{x}_T) = \mathcal{N}(\mathbf{x}_T; \mathbf{0}, \mathbf{I})$:

$$p_\theta(\mathbf{x}_{0:T}) := p(\mathbf{x}_T) \prod_{t=1}^T p_\theta(\mathbf{x}_{t-1} | \mathbf{x}_t), \quad p_\theta(\mathbf{x}_{t-1} | \mathbf{x}_t) := \mathcal{N}(\mathbf{x}_{t-1}; \boldsymbol{\mu}_\theta(\mathbf{x}_t, t), \boldsymbol{\Sigma}_\theta(\mathbf{x}_t, t)) \quad (1)$$

Mathematically

Training is performed by optimizing the usual variational bound on negative log likelihood:

$$\mathbb{E} [-\log p_{\theta}(\mathbf{x}_0)] \leq \mathbb{E}_q \left[-\log \frac{p_{\theta}(\mathbf{x}_{0:T})}{q(\mathbf{x}_{1:T}|\mathbf{x}_0)} \right] = \mathbb{E}_q \left[-\log p(\mathbf{x}_T) - \sum_{t \geq 1} \log \frac{p_{\theta}(\mathbf{x}_{t-1}|\mathbf{x}_t)}{q(\mathbf{x}_t|\mathbf{x}_{t-1})} \right] =: L \quad (3)$$

Mathematically

Efficient training is therefore possible by optimizing random terms of L with stochastic gradient descent. Further improvements come from variance reduction by rewriting L (3) as:

$$\mathbb{E}_q \left[\underbrace{D_{\text{KL}}(q(\mathbf{x}_T | \mathbf{x}_0) \parallel p(\mathbf{x}_T))}_{L_T} + \sum_{t>1} \underbrace{D_{\text{KL}}(q(\mathbf{x}_{t-1} | \mathbf{x}_t, \mathbf{x}_0) \parallel p_{\theta}(\mathbf{x}_{t-1} | \mathbf{x}_t))}_{L_{t-1}} \underbrace{- \log p_{\theta}(\mathbf{x}_0 | \mathbf{x}_1)}_{L_0} \right] \quad (5)$$

Mathematically

However, we found it beneficial to sample quality (and simpler to implement) to train on the following variant of the variational bound:

$$L_{\text{simple}}(\theta) := \mathbb{E}_{t, \mathbf{x}_0, \epsilon} \left[\left\| \epsilon - \epsilon_{\theta}(\sqrt{\bar{\alpha}_t} \mathbf{x}_0 + \sqrt{1 - \bar{\alpha}_t} \epsilon, t) \right\|^2 \right] \quad (14)$$

$$\alpha_t := 1 - \beta_t \text{ and } \bar{\alpha}_t := \prod_{s=1}^t \alpha_s,$$

The forward process variances β_t can be learned by reparameterization [33] or held constant as hyperparameters

$$\epsilon \sim \mathcal{N}(\mathbf{0}, \mathbf{I})$$

ϵ_{θ} as a learned gradient of the data density.

Algorithm: training

Algorithm 1 Training

1: **repeat**

2: $\mathbf{x}_0 \sim q(\mathbf{x}_0)$

3: $t \sim \text{Uniform}(\{1, \dots, T\})$

4: $\epsilon \sim \mathcal{N}(\mathbf{0}, \mathbf{I})$

5: Take gradient descent step on

$$\nabla_{\theta} \left\| \epsilon - \epsilon_{\theta}(\sqrt{\bar{\alpha}_t} \mathbf{x}_0 + \sqrt{1 - \bar{\alpha}_t} \epsilon, t) \right\|^2$$

6: **until** converged

Algorithm: sampling

Algorithm 2 Sampling

```
1:  $\mathbf{x}_T \sim \mathcal{N}(\mathbf{0}, \mathbf{I})$ 
2: for  $t = T, \dots, 1$  do
3:    $\mathbf{z} \sim \mathcal{N}(\mathbf{0}, \mathbf{I})$  if  $t > 1$ , else  $\mathbf{z} = \mathbf{0}$ 
4:    $\mathbf{x}_{t-1} = \frac{1}{\sqrt{\alpha_t}} \left( \mathbf{x}_t - \frac{1-\alpha_t}{\sqrt{1-\bar{\alpha}_t}} \boldsymbol{\epsilon}_\theta(\mathbf{x}_t, t) \right) + \sigma_t \mathbf{z}$ 
5: end for
6: return  $\mathbf{x}_0$ 
```

Unconditional sampling results



Figure 6: Unconditional CIFAR10 progressive generation ($\hat{\mathbf{x}}_0$ over time, from left to right). Extended samples and sample quality metrics over time in the appendix (Figs. 10 and 14).

Conditional sampling results



Figure 7: When conditioned on the same latent, CelebA-HQ 256×256 samples share high-level attributes. Bottom-right quadrants are \mathbf{x}_t , and other quadrants are samples from $p_\theta(\mathbf{x}_0 | \mathbf{x}_t)$.

Interpolations

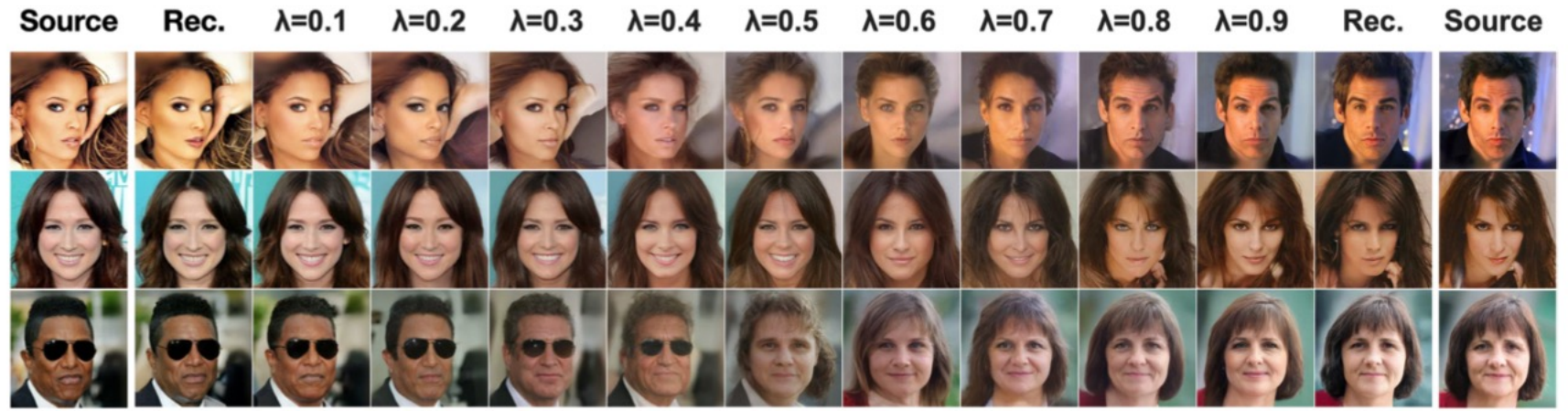
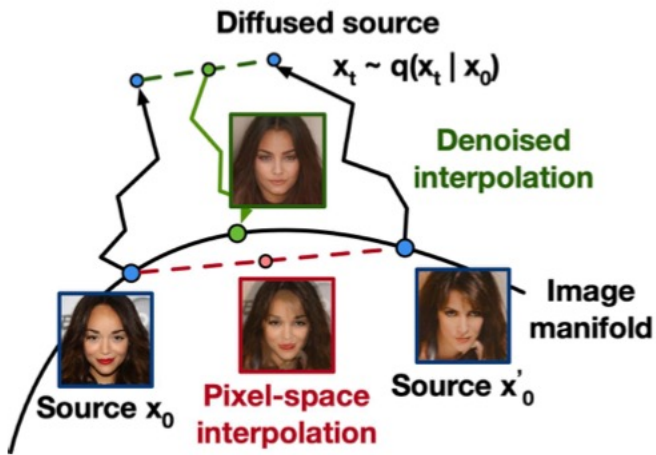


Figure 8: Interpolations of CelebA-HQ 256x256 images with 500 timesteps of diffusion.

Interpolations: math

We can interpolate source images $\mathbf{x}_0, \mathbf{x}'_0 \sim q(\mathbf{x}_0)$ in latent space using q as a stochastic encoder, $\mathbf{x}_t, \mathbf{x}'_t \sim q(\mathbf{x}_t|\mathbf{x}_0)$, then decoding the linearly interpolated latent $\bar{\mathbf{x}}_t = (1 - \lambda)\mathbf{x}_0 + \lambda\mathbf{x}'_0$ into image space by the reverse process, $\bar{\mathbf{x}}_0 \sim p(\mathbf{x}_0|\bar{\mathbf{x}}_t)$. In effect, we use the reverse process to remove artifacts from linearly interpolating corrupted versions of the source images, as depicted in Fig. 8

Questions